

# Boosting Higgs decays into gamma and a Z in the NMSSM

Geneviève Bélanger,<sup>1,\*</sup> Vincent Bizouard,<sup>1,†</sup> and Guillaume Chalons<sup>2,‡</sup>

<sup>1</sup>*LAPTh, Université de Savoie, CNRS, 9 Chemin de Bellevue,  
B.P. 110, F-74941 Annecy-le-Vieux, France*

<sup>2</sup>*LPSC, Université Grenoble-Alpes, CNRS/IN2P3,  
Grenoble INP, 53 rue des Martyrs, F-38026 Grenoble, France*

(Dated: June 30, 2018)

In this work we present the computation of the Higgs decay into a photon and a  $Z^0$  boson at the one-loop level in the framework of the Next-to-Minimal Supersymmetric Standard Model (NMSSM). The numerical evaluation of this decay width was performed within the framework of the `SloopS` code, originally developed for the Minimal Supersymmetric Standard Model (MSSM) but which was recently extended to deal with the NMSSM. Thanks to the high level of automation of `SloopS` all contributions from the various sector of the NMSSM are consistently taken into account, in particular the non-diagonal chargino and sfermion contributions. We then explored the NMSSM parameter space, using `HiggsBounds` and `HiggsSignals`, to investigate to what extent these signal can be enhanced.

## I. INTRODUCTION

The discovery of a 125 GeV Higgs boson at the LHC in July 2012 [1, 2], is a milestone in the road leading to the elucidation the ElectroWeak Symmetry Breaking (EWSB) riddle. Since then, its couplings to electroweak gauge bosons, third generation fermions and the loop-induced couplings to photon and gluons have been measured with an already impressive accuracy by the ATLAS and CMS collaborations [3, 4] during the 7 and 8 TeV runs. This great achievement was made possible since for a 125 GeV Higgs bosons many different production and decay channels are detectable at the LHC. A spin and parity analysis of the Higgs boson in the decays  $H \rightarrow \gamma\gamma$ ,  $H \rightarrow ZZ^*$  and  $H \rightarrow WW^*$  favor the  $J^P = 0^+$  hypothesis [5, 6].

The couplings of the Higgs to photons  $H\gamma\gamma$  and gluons  $Hgg$  are induced at the quantum level, even in the Standard Model (SM), and thus are interesting probes of New Physics (NP) since both the SM and NP contributions enter at the same level. On the one hand, the updated CMS analysis [7] gives a signal strength for the diphoton which is now compatible with the SM, compared to the previous one. On the other hand, the updated ATLAS analysis [8] still observes a slight excess of events in this channel but recent measurements of the  $H \rightarrow \gamma\gamma$  differential cross sections do not show significant disagreements with expectations from a SM Higgs [9].

The search for another important loop-induced Higgs decay channel,  $H \rightarrow \gamma Z^0$ , is also performed by the ATLAS and CMS experiments [10, 11]. Within the SM, the partial width

---

\*belanger@lapth.cnrs.fr

†bizouard@lapth.cnrs.fr

‡chalons@lpsc.in2p3.fr

for this channel,  $\Gamma_{\gamma Z}$ , is about two thirds of that for the diphoton decay and its measurement can also provide insights about the properties of the boson, such as its mass, spin and parity [12], thanks to a clean final state topology. No excess above SM predictions has been found in the 120-160 GeV mass range, and first limits on the Higgs boson production cross section times the  $H \rightarrow \gamma Z^0$  branching fraction have been derived [10, 11]. The collaborations set an upper limit on the ratio  $\Gamma_{\gamma Z}/\Gamma_{\gamma Z}^{\text{SM}} < 10$ . A measurement of  $\Gamma_{\gamma Z^0}$  can also provide insights about the underlying dynamics of the Higgs sector since new heavy charged particles can alter the SM prediction, just as for the  $H \rightarrow \gamma\gamma$  channel, without affecting the gluon-gluon fusion Higgs production cross section [13]. Moreover, the measurement of  $H \rightarrow \gamma Z^0$  and its rate compared to  $H \rightarrow \gamma\gamma$  is crucial for broadening our understanding of the EWSB pattern [14–16]. Testing the SM nature of this Higgs state and inspecting possible deviations in its coupling to SM particles will represent a major undertaking of modern particle physics and a probable probe of models going beyond the Standard Model (BSM).

Despite the fact that no significant deviation from the SM has been observed, there are many theoretical arguments and observations from astroparticle physics and cosmology supporting the fact that it cannot be the final answer for a complete description of Nature. If New Physics must enter the game, what the experimental results told us so far is that any BSM should exhibit decoupling properties. Among BSM, supersymmetry (SUSY) is probably the best motivated and most studied framework. Its minimal incarnation, the minimal supersymmetric standard model (MSSM), although possessing such a decoupling regime, relies heavily on the features of the stop sector to reproduce a 125 GeV Higgs boson; see [17–20]. The introduction of an additional gauge-singlet superfield  $S$  to the MSSM content, whose simplest version is dubbed as the Next-to-Minimal Supersymmetric Standard Model (NMSSM) [21, 22], relaxes such an upper bound and alters the dependence with respect to the stop sector. The singlet term provides an extra tree level contribution to the Higgs mass matrix such that the MSSM limit can be exceeded, already at the tree level [23–25]. The neutral CP-even Higgs sector is then enlarged with three states  $h_i^0$ , where  $i$  ranges from 1 to 3 and is ordered in increasing mass. In this context the lightest CP-even Higgs state might well be dominantly singlet with reduced couplings to the SM and thus could remain essentially invisible at colliders: the SM-like Higgs state would then be the second lightest and a small mixing effect with the singlet would in turn shift its mass towards slightly higher values. The NMSSM possesses another virtue, in addition to the ones of the MSSM: the so-called  $\mu$  problem of the MSSM [26] can be circumvented as it is dynamically generated once the singlet field gets a vacuum expectation value (vev) [21, 22]. All in all, the NMSSM now appears as more appealing than the MSSM and has received considerable attention [27–48].

In the present work, we investigate the  $\gamma Z^0$  decay channel of the SM-like Higgs boson  $h$  of the NMSSM and its correlation with  $H \rightarrow \gamma\gamma$ . We compute these two decay widths with the help of the automatic code `SloopS` [49, 50], initially designed to tackle one-loop calculations in the MSSM [51–54]. This code has been recently further developed to deal with the NMSSM extended field content and applied to Dark Matter [55–57] and Higgs phenomenology [58]. Thanks to this implementation, all the relevant particles running in the loops are properly taken into account, in particular the non-diagonal contributions due to the non-diagonal couplings of the  $Z$  boson to charginos and sfermions. Our results are consistent with those presented in [59]. As compared to [59], we perform a more thorough exploration on the parameter space of the NMSSM, in particular also considering the small  $\lambda$  region, and we compute the expected signal strengths for both the vector boson fusion

production mode (VBF) and the gluon fusion mode ( $gg$ ). In addition we impose the most recent collider constraints on the Higgs sector using `HiggsBounds`[60] and `HiggsSignals`[61] to require that one of the Higgses fits the properties of the particle observed at the LHC, thus illustrating that the most severe deviations from the SM expectations for  $H \rightarrow \gamma Z^0$  are already constrained. We further explicitly distinguish the case where the 125 GeV Higgs is the lightest or second lightest CP-even Higgs in the NMSSM.

This work is organized as follows. In the first part we quickly review the CP-even Higgs sector of NMSSM relevant for our work, and in the second part we discuss the calculation of the  $H \rightarrow \gamma\gamma(Z^0)$  partial widths and review the effects of SM and SUSY particles inside the loops. In the next section we present the implementation and the numerical evaluation of the partial width within `SloopS` and then we carry out a numerical investigation to explore to what extent the signal can be enhanced in the NMSSM after applying various experimental constraints. In the last section we draw our conclusions.

## II. CP-EVEN HIGGS SECTOR OF THE NMSSM

In the NMSSM superpotential the  $\mu$ -term involving the two Higgs doublet superfields  $\hat{H}_u$  and  $\hat{H}_d$  is absent and a gauge singlet superfield  $\hat{S}$  is added instead [21, 22]:

$$W_{\text{NMSSM}} = W_{\text{MSSM}}^{\mu=0} + \lambda \hat{S} \hat{H}_u \cdot \hat{H}_d \quad (1)$$

The MSSM  $\mu$  bilinear term has now been replaced by the trilinear coupling of the singlet with the two doublets and any dimensionful terms are forbidden by requiring the superpotential to be  $\mathbb{Z}_3$  symmetric. Once the singlet acquires a vev  $s = \langle S \rangle$ , an effective  $\mu$  term is generated with respect to the MSSM, which is then naturally of the order of the electroweak (EW) scale,

$$\mu_{\text{eff}} = \lambda s \quad (2)$$

The soft-SUSY breaking Lagrangian is also modified according to

$$\begin{aligned} -\mathcal{L}_{\text{soft}} &= m_{H_u}^2 |H_u|^2 + m_{H_d}^2 |H_d|^2 + m_S^2 |S|^2 \\ &+ (\lambda A_\lambda H_u \cdot H_d S + \frac{1}{3} \kappa A_\kappa S^3 + h.c.) \end{aligned} \quad (3)$$

where  $H_u \cdot H_d$  stands for the usual  $SU(2)$  product:  $X \cdot Y = X^T \varepsilon Y$  with  $\varepsilon = -i\sigma_2$ . Given  $M_Z$  and using conditions coming from the minimization of the Higgs potential, one can choose six independent parameters for the Higgs sector

$$\lambda, \kappa, A_\lambda, A_\kappa, \mu_{\text{eff}}, t_\beta \quad (4)$$

where  $t_\beta = \tan\beta = v_u/v_d$ , the ratio of the two Higgs doublet vevs:  $\langle H_u^0 \rangle = v_u$ ,  $\langle H_d^0 \rangle = v_d$ . From the superpotential in Eq. (1), one derives the tree-level Higgs potential containing the  $D$ -,  $F$ - and soft-SUSY breaking terms (we stick to real parameters):

$$\begin{aligned} V_0 &= (m_{H_u}^2 + \lambda^2 |S|^2) |H_u|^2 + (m_{H_d}^2 + \lambda^2 |S|^2) |H_d|^2 + |\lambda H_u \cdot H_d + \kappa S^2|^2 \\ &+ \frac{g'^2}{8} (|H_u|^2 - |H_d|^2)^2 + \frac{g^2}{8} \left[ (|H_u|^2 + |H_d|^2)^2 - 4|H_u \cdot H_d|^2 \right] \\ &+ m_S^2 |S|^2 + \left[ \lambda A_\lambda S H_u \cdot H_d + \frac{1}{3} \kappa A_\kappa S^3 + h.c. \right] \end{aligned} \quad (5)$$

with  $g'$  and  $g$  being the  $U(1)_Y$  and  $SU(2)_L$  couplings respectively. The parameters  $m_{H_u}^2, m_{H_d}^2$  and  $m_S^2$  can be traded for the vevs  $v_u, v_d, s$  through the minimization conditions of  $V_0$ . The neutral physical fields are obtained by expanding the full scalar potential Eq. (5) around the vev's as

$$H_d = \begin{pmatrix} v_d + (h_d^0 + ia_d^0)/\sqrt{2} \\ -H_d^- \end{pmatrix}, \quad H_u = \begin{pmatrix} H_u^+ \\ v_u + (h_u^0 + ia_u^0)/\sqrt{2} \end{pmatrix}, \quad S = s + (h_s^0 + ia_s^0)/\sqrt{2} \quad (6)$$

The  $3 \times 3$  symmetric CP-even Higgs mass matrix is derived by collecting the real parts and reads, in the basis  $(h_u^0, h_d^0, h_s^0)$ ,

$$\mathcal{M}_S^2 = \begin{pmatrix} M_Z^2 s_\beta^2 + \mu_{\text{eff}} B_{\text{eff}} c t_\beta & (\lambda^2 v^2 - M_Z^2/2) s_{2\beta} - \mu_{\text{eff}} B_{\text{eff}} & \lambda v(2\mu_{\text{eff}} s_\beta - (B_{\text{eff}} + \nu) c_\beta) \\ \cdot & M_Z^2 c_\beta^2 + \mu_{\text{eff}} B_{\text{eff}} t_\beta & \lambda v(2\mu_{\text{eff}} c_\beta - (B_{\text{eff}} + \nu) s_\beta) \\ \cdot & \cdot & \lambda^2 v^2 A_\lambda s_{2\beta}/2\mu_{\text{eff}} + \nu(A_\kappa + 4\nu) \end{pmatrix} \quad (7)$$

where we have traded the  $SU(2)_L \times U(1)_Y$  gauge couplings for the gauge boson masses through  $M_Z^2 = (g^2 + g'^2)v^2/2, M_W^2 = g^2 v^2/2$ . We used the short-hand notations  $\nu = \kappa s, B_{\text{eff}} = A_\lambda + \nu$  as well as  $\cos \beta = c_\beta, \sin \beta = s_\beta$  and so forth for trigonometric functions. The physical eigenstates  $h_i^0$  (with  $i = 1$  to 3) are obtained by diagonalizing Eq. (7) with an orthogonal matrix  $S_h$  such that  $\text{diag}(m_{h_1^0}^2, m_{h_2^0}^2, m_{h_3^0}^2) = S_h \mathcal{M}_S^2 S_h^{-1}$ . Although it is possible, as said in the Introduction, to reproduce a 125 GeV SM-like Higgs mass in the NMSSM already at the tree-level, radiative corrections (mostly from the stop sector) to the Higgs sector are significant [21, 62, 63] and should be taken into account. For this purpose, we computed the radiatively corrected Higgs masses using the publicly available code `NMSSMTools` [64–66].

### III. THE $H \rightarrow \gamma\gamma$ AND $H \rightarrow \gamma Z^0$ DECAY WIDTHS

The partial width  $\Gamma_{\gamma\gamma}$  and  $\Gamma_{\gamma Z}$  in the case of the CP-even  $h_i^0$  Higgs bosons can be written in SUSY generically as,

$$\Gamma_{\gamma\gamma}(h_i^0) = \frac{\alpha^2 G_F^2 m_{h_i^0}^3}{128\sqrt{2}\pi^3} \left| \sum_f \mathcal{A}_f^{\gamma\gamma} + \mathcal{A}_W^{\gamma\gamma} + \mathcal{A}_{H^\pm}^{\gamma\gamma} + \sum_{\tilde{f}} \mathcal{A}_{\tilde{f}}^{\gamma\gamma} + \mathcal{A}_{\chi^\pm}^{\gamma\gamma} \right|^2 \quad (8)$$

$$\Gamma_{\gamma Z}(h_i^0) = \frac{\alpha G_F^2 m_W^2 m_{h_i^0}^3}{64\pi^4} \left( 1 - \frac{m_Z^2}{m_{h_i^0}^2} \right) \left| \sum_f \mathcal{A}_f^{\gamma Z} + \mathcal{A}_W^{\gamma Z} + \mathcal{A}_{H^\pm}^{\gamma Z} + \sum_{\tilde{f}} \mathcal{A}_{\tilde{f}}^{\gamma Z} + \mathcal{A}_{\chi^\pm}^{\gamma Z} \right|^2 \quad (9)$$

The analytic expression for each amplitude  $\mathcal{A}_j$  ( $j = W, f, H^\pm, \tilde{f}, \chi^\pm$ ) can be found in [14, 59, 67]. For the sake of completeness, let us first discuss the SM-like contributions  $\mathcal{A}_W$  and  $\mathcal{A}_f$ . As the Higgs boson couples to SM particles proportionally to their mass, its couplings to neutral gauge bosons are dominantly mediated by the heaviest charged particles of the SM: the  $W^\pm$  boson and third generation quarks ( $f = t, b$ ). The growing of the couplings with the mass counterbalances the decrease of the triangle amplitudes with an increasing loop mass, thereby not decoupling the contribution of heavy particles. The remaining fermion contributions are much smaller, due to smaller masses. These two partial widths are therefore interesting probes of the number of heavy charged particles which can couple to the Higgs

boson. In both decay channels the  $W$  loops are by far the dominant ones and about 4.5 times larger than the top quark amplitude for a 125 GeV Higgs bosons for the  $\gamma\gamma$  channel and about one order of magnitude in the  $\gamma Z^0$  case [14]. However, the total width is significantly reduced by the destructive interference between the two contributions. The full two-loop corrections (EW+QCD) for the SM-like Higgs decay into  $\gamma\gamma$  and is under 2% [68] below the  $W^+W^-$  threshold. The complete QCD corrections at the three loop level are also known and were presented in [69]. For the  $\gamma Z^0$  decay width, the two loop QCD corrections to top quark loops were computed in [70] and the relative magnitude of the QCD correction to the partial width for a 125 GeV SM-like Higgs boson is below 0.3 %.

In SUSY theories, the additional superpartners of the SM particles do not couple to the Higgs boson proportionally to their masses, as the masses are generated through the soft-SUSY breaking Lagrangian and not the Higgs mechanism. Hence, these contributions are suppressed by the heavy masses running in the loops. However, if some of the superpartners' masses are not too large, most notably the lightest chargino and third generation squarks when the squark mixing angle is large, the decay channels can be affected and their contribution can enable a discrimination between the lightest SUSY and standard Higgs boson even in the decoupling regime [67]. Although the  $h_i^0 \rightarrow \gamma Z^0$  partial width is generically suppressed with respect to  $h_i^0 \rightarrow \gamma\gamma$ , this channel is of interest as the non-diagonal couplings of the Higgs and the  $Z^0$  gauge boson to sfermions  $\tilde{f}_1\tilde{f}_2$  and  $\tilde{\chi}_1^\mp\tilde{\chi}_2^\pm$  pairs are active. They are absent in the two-photon case due to the  $U(1)_{\text{QED}}$  gauge invariance. The complete analytical LO SUSY amplitudes can be found in [14, 59, 67]. The common lore is that these non-diagonal contributions are ignored since they are in general small for most purposes [67]. In the package `NMSSMTools` [64–66] the diagonal chargino loop contributions only are included and all sfermions contributions are missing. It was pointed out in [59] that sometimes they may play a role and that some numerical factors were missing in [14]. In the present work we computed these partial widths with the numerical code `SloopS`[49, 50] which automatically generates the one-loop amplitudes and shuns hand calculation errors thanks to internal checks like ultraviolet (UV) finiteness and gauge invariance. We now turn to the description of the numerical computation in the next section.

#### IV. NUMERICAL EVALUATION OF $\Gamma_{\gamma\gamma}$ AND $\Gamma_{\gamma Z}$ WITH SLOOPS

In `SloopS`, the complete spectrum and set of vertices are generated at the tree level through the `LanHEP` package [71–73]. The complete set of Feynman rules is then derived automatically and passed to the bundle `FeynArts/FormCalc/LoopTools` [74–76] (that we denote as `FFL`). A powerful feature of `SloopS` is the ability to check not only the UV finiteness check as provided by `FFL`, but also the gauge independence of the result through a generalized gauge fixing Lagrangian, which was adapted to the NMSSM [55]. The gauge-fixing Lagrangian can be written in a general form:

$$\mathcal{L}_{GF} = -\frac{1}{\xi_W} F^+ F^- - \frac{1}{2\xi_Z} |F^Z|^2 - \frac{1}{2\xi_A} |F^A|^2 \quad (10)$$

For the  $\Gamma_{\gamma\gamma}$  and  $\Gamma_{\gamma Z}$  decay width only the nonlinear form of  $F^\pm$  is of relevance and is given by<sup>1</sup>

$$F^+ = \left( \partial_\mu - ie\tilde{\alpha}A_\mu - igc_W\tilde{\beta}Z_\mu \right) W^{\mu+} + i\xi_W \frac{g}{2} \left( v + \sum_{i=1}^3 \tilde{\delta}_i h_i^0 \right) G^+ \quad (11)$$

The parameters  $\tilde{\alpha}$ ,  $\tilde{\beta}$  and  $\tilde{\delta}_i$  are dubbed as nonlinear gauge (NLG) parameters and  $G^\pm$  are the charged Goldstone fields. We recover the usual 't Hooft-Feynman gauge by setting these parameters to vanishing values. The ghost Lagrangian  $\mathcal{L}_{Gh}$  is established by requiring that the full Lagrangian is invariant under BRST transformations.<sup>2</sup> The gauge dependence is in turn transferred from the vector boson propagators to a modification of the ghost-Goldstone-vector boson vertices (see for example [77]). Numerically the gauge invariance check is performed by varying the parameters  $\tilde{\alpha}$ ,  $\tilde{\beta}$  and  $\tilde{\delta}_i$ .

Similarly to the MSSM, radiative corrections to the Higgs masses in the NMSSM can be relatively large (see e.g [62] and references therein) and thus significantly affect the kinematics of the decay. As said previously, we used `NMSSMTools` to compute the Higgs spectrum and rotation matrices. Since the Higgs spectrum and parameters entering the Higgs potential in Eq. (5) are not independent quantities, a shift on the tree level Higgs masses also results in a shift of the parameters and thus on the Higgs-to-Higgs couplings. Therefore, to parametrize the radiative corrections to the Higgs masses and couplings we make use of the effective Lagrangian devised in [58] and given by

$$V_{\text{eff}} = V_0 + V_{\text{rad}} \quad (12)$$

where  $V_0$  is the same as Eq.(5) and

$$V_{\text{rad}} = \frac{\lambda_1}{2}|H_d|^4 + \frac{\lambda_2}{2}|H_u|^4 + \lambda_3|H_u|^2|H_d|^2 + \lambda_4|H_u \cdot H_d|^2 + \bar{\kappa}^2|S|^4 + \frac{1}{3}(\bar{A}_S S^3 + h.c.) \\ + \lambda_P^u |S|^2 |H_u|^2 + \lambda_P^d |S|^2 |H_d|^2 + [A_{ud} S H_u \cdot H_d + \lambda_P^M S^{*2} H_u \cdot H_d + h.c.] \quad (13)$$

Once the spectrum and mixing matrices are known from `NMSSMTools` we solve for the  $\lambda s^3$  using equations derived from the effective Higgs mass matrices extracted from Eq. (12). We refer to [58] for further details concerning the extracting procedure of the  $\lambda$  parameters. This procedure then ascertains the gauge independence of the computation. This was explicitly demonstrated analytically and numerically in [58] for the partial width  $h_i^0 \rightarrow \gamma\gamma$ . The nonlinear gauge-fixing Lagrangian possesses another virtue: setting particular values to the NLG parameters can cancel specific vertices. For the case at hand, with the peculiar choice  $\tilde{\alpha} = -1$  the coupling  $\gamma W^\pm G^\mp$  is absent due to an underlying  $U(1)_{\text{QED}}$  symmetry conserving gauge-fixing function  $F^\pm$  and less diagrams have to be considered. This property is therefore a welcomed feature and was employed to simplify the analytic calculation of  $H \rightarrow \gamma\gamma$  in [78, 79]. Although in such a gauge the calculation of the SM-like amplitude of  $\Gamma_{\gamma Z}$  is not easily translated from  $\Gamma_{\gamma\gamma}$ , since the vanishing of the  $\gamma W^\pm G^\mp$  vertex introduces an asymmetric treatment of the photon and the  $Z^0$  boson [80], the evaluation of the  $Z - \gamma$  transition diagram  $\Pi_{\gamma Z}(0)$  is not needed. Indeed, for  $\tilde{\alpha} = -1$  this mixing self-energy vanishes

<sup>1</sup> The other gauge-fixing functions  $F^Z$  and  $F^A$  can be kept in the usual  $R_\xi$  form. The complete expressions can be found in [55]. For practical purposes we set  $\xi_{W,Z,A} = 1$ .

<sup>2</sup> The BRST transformations for the gauge fields can be found in [77] and for the scalar fields in [55].

<sup>3</sup> We denote generically as “ $\lambda$ ” any parameter entering Eq. (13).

at  $q^2 = 0$  thanks to, once more, the fact that  $F^\pm$  preserves the  $U(1)_{\text{QED}}$  gauge symmetry [77]. This is of importance for our numerical evaluation of  $\Gamma_{\gamma Z}$  since we do not generate diagrams with external wave function correction and the introduction of the field-renormalization constant  $\delta Z_{Z\gamma}^{1/2} = -\Pi_{\gamma Z^0}^T(0)/M_Z^2$  would not be needed in such a gauge. In a general nonlinear gauge this transition is crucial to maintaining the UV finiteness and the gauge invariance of the result. We thoroughly checked this feature numerically by varying the NLG parameters  $\tilde{\alpha}$ ,  $\tilde{\beta}$  and  $\tilde{\delta}_i$ .

## V. NUMERICAL INVESTIGATION

Although the properties of the Higgs boson observed at the LHC are compatible with the SM predictions [1, 81], the precise measurements of all its decay channels can give some crucial information on new physics. In this analysis we examine the expectations for the decay  $h_i^0 \rightarrow \gamma Z^0$  in the framework of the NMSSM after taking into account the constraints on the Higgs observed at the LHC. In particular we quantify the importance of the sfermions and non-diagonal charginos contributions discussed in the previous section. For this we explore the parameter space of the NMSSM with emphasis on the regions which could lead potentially to large corrections, those with light charginos and/or light stop.

The chargino mass matrix is given by,

$$\begin{pmatrix} M_2 & gv_u \\ gv_d & \mu_{eff} \end{pmatrix} \quad (14)$$

while the stop mass matrix in the  $(\tilde{t}_R, \tilde{t}_L)$  basis, reads

$$\begin{pmatrix} m_{\tilde{U}_3}^2 + h_t^2 v_u^2 - (v_u^2 - v_d^2) \frac{g'^2}{3} & h_t(A_t v_u - \mu_{eff} v_d) \\ h_t(A_t v_u - \mu_{eff} v_d) & m_{\tilde{Q}_3}^2 + h_t^2 v_u^2 + (v_u^2 - v_d^2) \left( \frac{g'^2}{12} - \frac{g^2}{4} \right) \end{pmatrix} \quad (15)$$

where  $M_2$  is the SU(2) gaugino mass,  $m_{\tilde{Q}_3}, m_{\tilde{U}_3}$  are the soft masses for the stops and  $A_t$  is the stop trilinear mixing. Since  $h_t$  is of the order 1, the mixing between both stops can be important. The large mixing can lead to large radiative corrections to the SM-like Higgs mass and to one of the stops being quite light. Thus, the main squark contribution to the Higgs loop-induced decays ( $\gamma\gamma, \gamma Z^0$  and  $gg$ ) is coming from the stop sector.

To restrict the number of free parameters of the phenomenological NMSSM, we perform a scan over only the parameters most relevant for the Higgs mass (Eq. 7) and couplings, specifically those of the chargino, squark and Higgs sectors which we take in the following range:

$$\begin{aligned} 100 \text{ GeV} &< \mu &< 500 \text{ GeV} \\ 100 \text{ GeV} &< M_2 &< 1000 \text{ GeV} \\ 0 \text{ GeV} &< t_\beta &< 20 \\ 0 &< \lambda, \kappa &< 0.7 \\ 100 \text{ GeV} &< A_\lambda &< 1000 \text{ GeV} \\ -1000 \text{ GeV} &< A_\kappa &< -100 \text{ GeV} \\ -3000 \text{ GeV} &< A_t &< 3000 \text{ GeV} \\ 400 \text{ GeV} &< m_{\tilde{Q}_3}, m_{\tilde{U}_3} &< 2000 \text{ GeV} \end{aligned}$$

We assume that all squarks of the first and second generations are heavy ( $m_{\tilde{Q}_i} = m_{\tilde{u}_i} = m_{\tilde{d}_i} = 2$  TeV) as well as the right-handed sbottom mass,  $m_{\tilde{d}_3} = 2$  TeV, since they do not play an important role in Higgs physics. We also assume that all sleptons are heavy,  $m_{\tilde{L}_i} = m_{\tilde{\nu}_i} = 2$  TeV<sup>4</sup>, as well as the gluino,  $M_3 = 1.5$  TeV. The most important LHC constraints on supersymmetric particles are then automatically satisfied. Finally, we set  $M_1 = 150$  GeV, the exact value of the neutralino LSP is not very important for our analysis, provided the neutralino is too heavy for the Higgs to decay invisibly. However, the value of  $M_1$  could be adjusted to ensure that the limit on the stop mass from the LHC is satisfied (the limit on the lightest stop can easily be avoided when  $m_{\tilde{t}_1} - m_{\tilde{\chi}_1} < m_t$ ) [82, 83]. Note that we concentrate on small values of  $\tan\beta$  since it is the region where the Higgs sector can differ significantly from that of the MSSM. In this region one can find large deviations in the  $h_i^0 \rightarrow \gamma\gamma$  decay [28] due in particular to the singlet component of the Higgs. Thus, large deviations are also expected for  $h_i^0 \rightarrow \gamma Z^0$ .

In the NMSSM, either of the light scalar,  $h_1^0$  or  $h_2^0$ , could be the one observed at the LHC with a mass of 125 GeV: we consider both possibilities. We use `NMSSMTools` to compute the supersymmetric spectrum and to impose constraints on the parameter space<sup>5</sup>, specifically: the large electron positron (LEP) collider constraints on Higgs and chargino masses as well as the constraint that there be no unphysical global minimum on the Higgs potential. We select only the points with one Higgs in the mass range 122 – 128 GeV. Finally, we impose the collider constraints on the Higgs sector from `HiggsBounds` [60] and require that one Higgs fits the properties of the particle observed at the LHC using `HiggsSignals` [61]. For these two codes, we choose a theoretical uncertainty of 2 GeV for the Higgs masses. The allowed points are those for which  $\chi^2 < \chi_{\text{bestfit}}^2 + 18.3$  corresponding to the 95% confidence level (C.L) for ten free parameters. Note that the best fit point is slightly better than the SM.

First, we checked whether sfermions and non-diagonal charginos contributions have a significant impact on the the process  $h_i^0 \rightarrow \gamma Z^0$ ; for this we calculate the following ratio :

$$R = \frac{\Gamma(h_i^0 \rightarrow \gamma Z^0)_{total}}{\Gamma(h_i^0 \rightarrow \gamma Z^0)_{restricted}} \quad , \quad (16)$$

where  $\Gamma(h_i^0 \rightarrow \gamma Z^0)_{total}$  is the decay width calculated with all the possible particles in the loops, and  $\Gamma(h_i^0 \rightarrow \gamma Z^0)_{restricted}$  is the one calculated by omitting sfermions and non-diagonal charginos contributions in the loop.

The results for the ratio are shown in Fig. 1. In both cases, the ratio is plotted as a function of the mass of the corresponding Higgs boson. We notice that, for most of the points, the effect is less than  $\sim 10\%$ . In fact, the main effect is coming from the chargino contributions; we have checked that with only the sfermionic contribution the effect is less than 5%. However, for a few points, the variation can be as high as 70% in the case of  $h_2^0$ . These large deviations are found for points for which  $h_2^0$  is almost singlet : in this case

<sup>4</sup> We have made additional scans to check the impact of varying the parameters of the stau sector. Corrections to  $h_i^0 \rightarrow \gamma Z^0$  lie below a few percent except for very light staus (below the LEP limit). We expect that for values of  $\tan\beta$  much larger than those considered here, one can get large enhancement to the  $\gamma Z^0$  branching ratio as was shown previously for the  $h \rightarrow \gamma\gamma$  in the MSSM [13].

<sup>5</sup> See also [63] for a full one-loop calculation of the Higgs boson spectrum in the real and complex NMSSM using a mixed DR and OS renormalization scheme and for a comparison between the different methods.

the partial decay width is suppressed since the  $W$  contribution becomes negligible and the chargino (higgsino) contribution can become relatively more important. Note that for the singlet case the total decay width is also suppressed, leading to a branching ratio that can be either enhanced or suppressed relative to the SM. However, most of these points are excluded by LHC constraints on the Higgs sector.

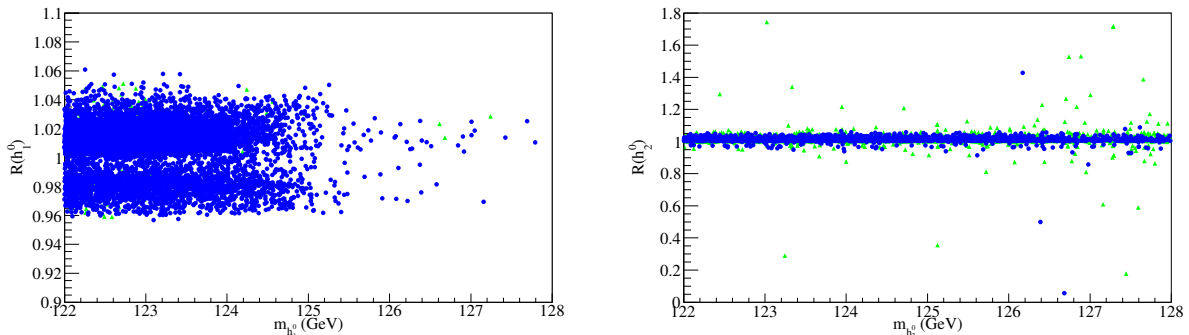


FIG. 1: Ratio of the decay width of  $h_1^0 \rightarrow \gamma Z^0$  (left panel) and  $h_2^0 \rightarrow \gamma Z^0$  (right panel) with all possible particles in the loop by the one without sfermions nor non diagonal  $Z$ -charginos contributions as a function of the mass of  $h_i^0$ . Blue points are allowed and green triangles are excluded by LHC constraints on the Higgs.

We next consider the expectations for the  $h_i^0 \rightarrow \gamma Z^0, \gamma\gamma$  branching ratios in the NMSSM as compared to the SM when including all contributions. The case where  $h_1^0$  is near 125 GeV leads to only mild variations of the  $\gamma Z^0$  branching ratio - typically  $\approx 10\%$ . In a few cases however deviations as large as 25% can be found; typically they are found when  $h_1^0$  has a significant singlet component. In all cases we found a strong correlation to the  $h_1^0 \rightarrow \gamma\gamma$  branching ratio (within 10%). The two-photon mode should therefore provide a better probe of new physics effects in the NMSSM considering it can be measured with a much better precision.

The results for  $h_2^0 \rightarrow \gamma Z^0, \gamma\gamma$  are more interesting. Figure 2 shows the branching ratio  $h_2^0 \rightarrow \gamma Z^0$  as compared to the SM value as a function of the mass of the lightest Higgs boson (recall that for these points  $122\text{GeV} < m_{h_2^0} < 128\text{GeV}$ ). Although the bulk of the points are centered around the SM value, large deviations can occur, in particular when the lightest Higgs is near 120 GeV. In this case  $h_2^0$  has a large singlet component and the  $Br(h_2^0 \rightarrow \gamma Z^0)$  can be up to 4 times larger than the SM or suppressed by more than two orders of magnitude. Note that most of these points are excluded by the LHC constraints as implemented in `HiggsSignals` either because the production of the singlet Higgs deviates significantly from the SM and/or the corresponding  $\gamma\gamma$  channel which is correlated with  $\gamma Z^0$  is incompatible with current measurements. Nevertheless, we found few points that satisfy the `HiggsSignals` constraints even though the  $h_2^0$  is almost a pure singlet and thus has non SM couplings; see the empty circles in Fig. 2 which have  $S_{h_{23}} > 0.9$ . The reason why such points avoid the LHC constraints is that they correspond to cases where  $h_1^0$  and  $h_2^0$  are almost degenerate and the superposition of the signal of both Higgs bosons is what is observed at the LHC ( $h_1^0$  is mainly doublet and SM-like).

The branching ratio  $h_2^0 \rightarrow \gamma Z^0$  can also be strongly suppressed when  $m_{h_1^0} < 60$  GeV and a new decay channel,  $h_2^0 \rightarrow h_1^0 h_1^0$ , opens up, thus significantly increasing the total width; see Fig. 2. Points with a large suppression are however incompatible with the LEP and LHC

constraints.

Finally, we comment on the correlation between the  $h_2^0 \rightarrow \gamma Z^0$  and  $h_2^0 \rightarrow \gamma\gamma$  channels displayed in Fig. 2, right panel. As for the case of  $h_1^0$ , both channels are strongly correlated. The correlation breaks down when  $h_2^0$  has a strong singlet component and mainly for points with suppressed  $\gamma Z^0/\gamma\gamma$  branching ratios that are to a large extent excluded by LHC constraints.

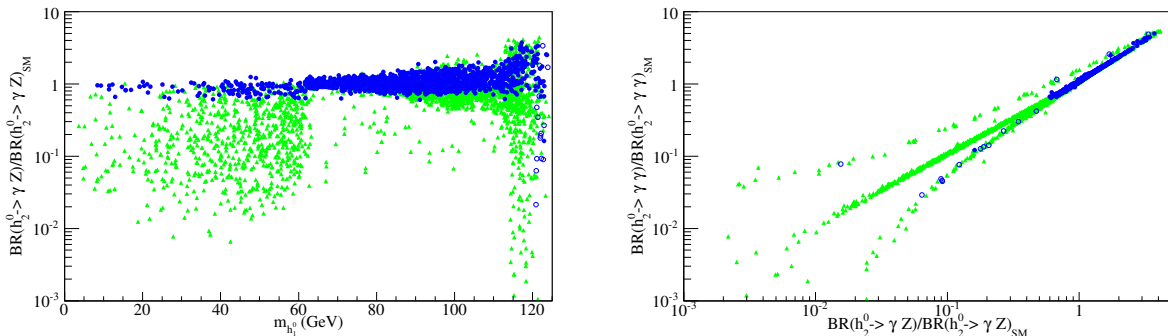


FIG. 2: Left panel : Branching ratio of  $h_2^0$  in  $\gamma Z^0$  in the NMSSM relative to the SM as a function of the mass of  $h_1^0$ . The green triangles correspond to points excluded at the 95% C.L. by HiggsBounds and HiggsSignals. The empty blue points correspond to  $Sh_{23} > 0.9$ . Right panel : Correlation between the reduced branching ratios  $h_2^0 \rightarrow \gamma Z^0$  and  $h_2^0 \rightarrow \gamma\gamma$ .

The LHC collaborations will not directly measure the branching ratio but the signal strengths ( $\mu$ ) for gluon fusion (gg) and vector boson fusion (VBF) production modes in the  $\gamma Z^0$  channel. The predictions for the signal strength in the gluon fusion mode are shown in Fig. 3 for  $h_2^0$  as a function of the scalar mixing  $Sh_{23}$ . Three regions present an enhancement as compared to the SM; they correspond to (a)  $Sh_{23} < -0.5$ , (b)  $Sh_{23} > 0.7$  and (c)  $Sh_{23} \approx 0.4$ . In all three cases,  $h_2^0$  has significant singlet and doublet components and its couplings to u-type quarks and gauge bosons are somewhat suppressed while those couplings to d-type quarks and leptons are strongly suppressed. As a result, the total width of  $h_2^0$  is much reduced and the branching ratio into  $WW, ZZ, \gamma\gamma, gg$  and  $\gamma Z^0$  are all larger than in the SM. The signal strength in the VBF mode is mostly correlated with that in the gluon fusion mode, although for some points the VBF is suppressed by more than a factor 2 as compared to the gluon fusion mode; see Fig. 3 right panel. In particular, note that the enhancement in the gluon fusion mode ( $\mu_{gg} > 1$ ) is more important than in the VBF mode. We had also mentioned that for  $Sh_{23} > 0.9$  which corresponds to a  $h_2^0$  that is dominantly singlet, the  $h_2^0 \rightarrow \gamma Z^0$  branching ratio could still be enhanced; however, the singlet coupling to gauge bosons becomes very small so that the VBF production mode is suppressed and to a lesser extent also the gluon fusion production mode, making it difficult to probe this dominantly singlet Higgs at the LHC.

## VI. CONCLUSION

We have performed a complete computation of the branching ratio into  $\gamma Z^0$  of both of the two lightest CP-even Higgs in the NMSSM using SloopS. Compared to previous work [59], in our scans we did not consider the large lambda regime only, but the full range of lambda values not producing a Landau pole before the grand unified theory scale. Moreover,

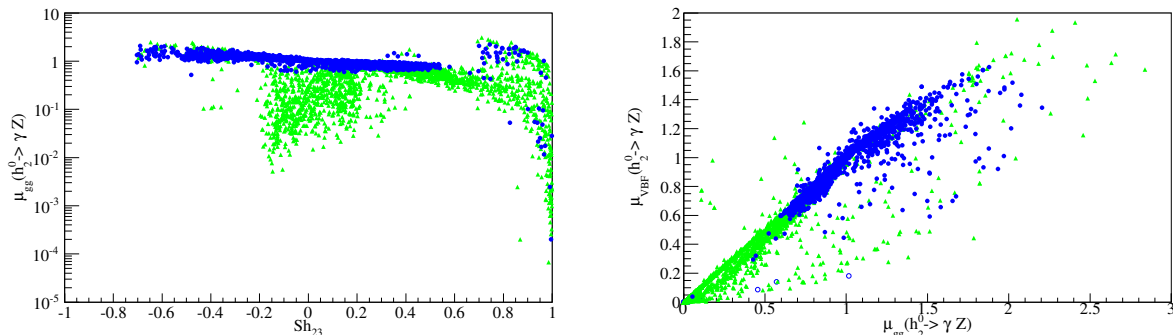


FIG. 3: Left panel : Signal strength for  $h_2^0 \rightarrow \gamma Z^0$  for gluon gluon fusion production with respect to  $Sh_{23}$ . Right panel: Correlation between the gg and VBF signal strengths. Same color code as Fig. 2

we investigated to what extent the signal can be enhanced knowing the measurements of the LHC on the Higgs boson signal strength. Also, strictly concerning the calculation of the decay rate, we made use of a modified Higgs boson potential to be able to use the corrected Higgs boson masses in the kinematics of the process while maintaining gauge invariance; this was checked thoroughly thanks to the implementation of a non-linear gauge fixing [58]. We found that the previously neglected contributions of charginos and stops (as well as staus) generally lie below 10%. Exploring the parameter space of the NMSSM, we found that  $h_1^0 \rightarrow \gamma Z^0$  did not vary much from the SM expectations while regions with a large enhancement (suppression) of  $h_2^0 \rightarrow \gamma Z^0$  were possible, especially when  $h_2^0$  had a significant singlet component. However, most of these scenarios are constrained by measurements of the 125 GeV Higgs boson at the LHC since the singlet component significantly changes the coupling of  $h_2^0$  to gauge bosons and fermions (in particular b quarks). We conclude that given the correlation between the  $\gamma\gamma$  and  $\gamma Z^0$  branching ratios expected in the NMSSM, a better measurement of the former at the next LHC run - together with a higher precision on other standard decay channels - will further constrain the range of values expected for  $h \rightarrow \gamma Z^0$ . Nevertheless an independent measurement of  $h \rightarrow \gamma Z^0$  is useful in probing BSM physics; for example, a large deviation from the SM expectations not correlated with a similar deviation in the  $\gamma\gamma$  mode would put strong constraints on the NMSSM (and other MSSM-like models). Furthermore, a suppressed signal strength in the VBF mode relative to the gluon fusion mode is characteristic of the partially singlet Higgs in the NMSSM.

## VII. ACKNOWLEDGEMENTS

We thank Fawzi Boudjema, Béranger Dumont, Guillaume Drieu La Rochelle, Alexander Pukhov and Chris Wymant for useful discussions. We also thank Tim Stefaniak for providing useful information on `HiggsSignals`. Partial funding from the French ANR, project DMAstroLHC, ANR-12-BS05-0006, and by the European Commission through the HiggsTools Initial Training Network, Grant No. PITN-GA-2012-316704, is gratefully acknowledged. The work of G.C is supported by the Theory-LHC-France initiative of the CNRS/IN2P3.

- 
- [1] G. Aad et al. (ATLAS Collaboration), Phys.Lett. **B716**, 1 (2012), 1207.7214.
  - [2] S. Chatrchyan et al. (CMS Collaboration), Phys.Lett. **B716**, 30 (2012), 1207.7235.
  - [3] ATLAS-CONF-2013-034 (2013).
  - [4] CMS-PAS-HIG-13-005 (2013).
  - [5] G. Aad et al. (ATLAS Collaboration), Phys.Lett. **B726**, 120 (2013), 1307.1432.
  - [6] S. Chatrchyan et al. (CMS Collaboration), Phys.Rev.Lett. **110**, 081803 (2013), 1212.6639.
  - [7] CMS-PAS-HIG-13-001 (2013).
  - [8] ATLAS-CONF-2013-012 (2013).
  - [9] ATLAS-CONF-2013-072 (2013).
  - [10] S. Chatrchyan et al. (CMS Collaboration), Phys.Lett. **B726**, 587 (2013), 1307.5515.
  - [11] Tech. Rep. ATLAS-CONF-2013-009, CERN, Geneva (2013).
  - [12] J. S. Gainer, W.-Y. Keung, I. Low, and P. Schwaller, Phys.Rev. **D86**, 033010 (2012), 1112.1405.
  - [13] M. Carena, S. Gori, N. R. Shah, and C. E. Wagner, JHEP **1203**, 014 (2012), 1112.3336.
  - [14] A. Djouadi, V. Driesen, W. Hollik, and A. Kraft, Eur.Phys.J. **C1**, 163 (1998), hep-ph/9701342.
  - [15] A. Djouadi, Phys.Rept. **457**, 1 (2008), hep-ph/0503172.
  - [16] B. A. Kniehl, Phys.Rept. **240**, 211 (1994).
  - [17] P. Draper, P. Meade, M. Reece, and D. Shih, Phys.Rev. **D85**, 095007 (2012), 1112.3068.
  - [18] T. Hahn, S. Heinemeyer, W. Hollik, H. Rzehak, and G. Weiglein, Phys.Rev.Lett **112**, 141801 (2014), 1312.4937.
  - [19] O. Buchmueller, R. Cavanaugh, A. De Roeck, M. Dolan, J. Ellis *et. al*, 1312.5250.
  - [20] O. Buchmueller, M. Dolan, J. Ellis, T. Hahn, S. Heinemeyer *et. al*, Eur.Phys.J **C74**, 2809 (2014), 1312.5233.
  - [21] U. Ellwanger, C. Hugonie, and A. M. Teixeira, Phys.Rept. **496**, 1 (2010), 0910.1785.
  - [22] M. Maniatis, Int.J.Mod.Phys. **A25**, 3505 (2010), 0906.0777.
  - [23] R. Barbieri, L. J. Hall, Y. Nomura, and V. S. Rychkov, Phys.Rev. **D75**, 035007 (2007), hep-ph/0607332.
  - [24] U. Ellwanger and C. Hugonie, Mod.Phys.Lett. **A22**, 1581 (2007), hep-ph/0612133.
  - [25] U. Ellwanger, G. Espitalier-Noel, and C. Hugonie, JHEP **1109**, 105 (2011), 1107.2472.
  - [26] J. E. Kim and H. P. Nilles, Phys.Lett. **B138**, 150 (1984).
  - [27] L. J. Hall, D. Pinner, and J. T. Ruderman, JHEP **1204**, 131 (2012), 1112.2703.
  - [28] U. Ellwanger, JHEP **1203**, 044 (2012), 1112.3548.
  - [29] A. Arvanitaki and G. Villadoro, JHEP **1202**, 144 (2012), 1112.4835.
  - [30] S. King, M. Muhlleitner, and R. Nevzorov, Nucl.Phys. **B860**, 207 (2012), 1201.2671.
  - [31] Z. Kang, J. Li, and T. Li, JHEP **1211**, 024 (2012), 1201.5305.
  - [32] J.-J. Cao, Z.-X. Heng, J. M. Yang, Y.-M. Zhang, and J.-Y. Zhu, JHEP **1203**, 086 (2012), 1202.5821.
  - [33] U. Ellwanger and C. Hugonie, Adv.High Energy Phys. **2012**, 625389 (2012), 1203.5048.
  - [34] K. S. Jeong, Y. Shoji, and M. Yamaguchi, JHEP **1209**, 007 (2012), 1205.2486.
  - [35] L. Randall and M. Reece, JHEP **1308**, 088 (2013), 1206.6540.
  - [36] R. Benbrik, M. Gomez Bock, S. Heinemeyer, O. Stal, G. Weiglein, et al., Eur.Phys.J. **C72**, 2171 (2012), 1207.1096.
  - [37] B. Kyae and J.-C. Park, Phys.Rev. **D87**, 075021 (2013), 1207.3126.

- [38] K. Agashe, Y. Cui, and R. Franceschini, *JHEP* **1302**, 031 (2013), 1209.2115.
- [39] G. Bélanger, U. Ellwanger, J. F. Gunion, Y. Jiang, S. Kraml, et al., *JHEP* **1301**, 069 (2013), 1210.1976.
- [40] Z. Heng, *Adv. High Energy Phys.* **2012**, 312719 (2012), 1210.3751.
- [41] K. Choi, S. H. Im, K. S. Jeong, and M. Yamaguchi, *JHEP* **1302**, 090 (2013), 1211.0875.
- [42] S. King, M. Muehlleitner, R. Nevzorov, and K. Walz, *Nucl.Phys.* **B870**, 323 (2013), 1211.5074.
- [43] T. Gherghetta, B. von Harling, A. D. Medina, and M. A. Schmidt, *JHEP* **02**, 032 (2013), 1212.5243.
- [44] T. Cheng, J. Li, T. Li, and Q.-S. Yan (2013), 1304.3182.
- [45] R. Barbieri, D. Buttazzo, K. Kannike, F. Sala, and A. Tesi, *Phys.Rev.* **D87**, 115018 (2013), 1304.3670.
- [46] M. Badziak, M. Olechowski, and S. Pokorski, *JHEP* **1306**, 043 (2013), 1304.5437.
- [47] T. Cheng and T. Li, *Phys.Rev.* **D88**, 015031 (2013), 1305.3214.
- [48] E. Hardy, *JHEP* **1310**, 133 (2013), 1306.1534.
- [49] N. Baro, F. Boudjema, and A. Semenov, *Phys.Rev.* **D78**, 115003 (2008), 0807.4668.
- [50] N. Baro and F. Boudjema, *Phys.Rev.* **D80**, 076010 (2009), 0906.1665.
- [51] F. Boudjema, A. Semenov, and D. Temes, *Phys.Rev.* **D72**, 055024 (2005), hep-ph/0507127.
- [52] N. Baro, F. Boudjema, and A. Semenov, *Phys.Lett.* **B660**, 550 (2008), 0710.1821.
- [53] N. Baro, G. Chalons, and S. Hao, *AIP Conf.Proc.* **1200**, 1067 (2010), 0909.3263.
- [54] N. Baro, F. Boudjema, G. Chalons, and S. Hao, *Phys.Rev.* **D81**, 015005 (2010), 0910.3293.
- [55] G. Chalons and A. Semenov, *JHEP* **1112**, 055 (2011), 1110.2064.
- [56] G. Chalons (2012), 1204.4591.
- [57] G. Chalons, M. J. Dolan, and C. McCabe, *JCAP* **1302**, 016 (2013), 1211.5154.
- [58] G. Chalons and F. Domingo, *Phys.Rev.* **D86**, 115024 (2012), 1209.6235.
- [59] J. Cao, L. Wu, P. Wu, and J. M. Yang, *JHEP* **1309**, 043 (2013), 1301.4641.
- [60] P. Bechtle, O. Brein, S. Heinemeyer, O. Stål, T. Stefaniak, et al. (2013), 1311.0055.
- [61] P. Bechtle, S. Heinemeyer, O. Stål, T. Stefaniak, and G. Weiglein (2013), 1305.1933.
- [62] G. Degrossi and P. Slavich, *Nucl.Phys.* **B825**, 119 (2010), 0907.4682.
- [63] J. Baglio, R. Grober, M. Muehlleitner, D. Nhung, H. Rzehak, et al. (2013), 1312.4788.
- [64] U. Ellwanger, J. F. Gunion, and C. Hugonie, *JHEP* **0502**, 066 (2005), hep-ph/0406215.
- [65] U. Ellwanger and C. Hugonie, *Comput.Phys.Commun.* **175**, 290 (2006), hep-ph/0508022.
- [66] U. Ellwanger and C. Hugonie, *Comput.Phys.Commun.* **177**, 399 (2007), hep-ph/0612134.
- [67] A. Djouadi, *Phys.Rept.* **459**, 1 (2008), hep-ph/0503173.
- [68] G. Passarino, C. Sturm, and S. Uccirati, *Phys.Lett.* **B655**, 298 (2007), 0707.1401.
- [69] P. Maierhofer and P. Marquard, *Phys.Lett.* **B721**, 131 (2013), 1212.6233.
- [70] M. Spira, A. Djouadi, and P. Zerwas, *Phys.Lett.* **B276**, 350 (1992).
- [71] A. Semenov, *Nucl.Instrum.Meth.* **A389**, 293 (1997).
- [72] A. Semenov, *Comput.Phys.Commun.* **115**, 124 (1998).
- [73] A. Semenov (2010), 1005.1909.
- [74] T. Hahn and M. Perez-Victoria, *Comput.Phys.Commun.* **118**, 153 (1999), hep-ph/9807565.
- [75] T. Hahn, *Comput.Phys.Commun.* **140**, 418 (2001), hep-ph/0012260.
- [76] T. Hahn, *Nucl.Phys.Proc.Suppl.* **135**, 333 (2004), hep-ph/0406288.
- [77] G. Bélanger, F. Boudjema, J. Fujimoto, T. Ishikawa, T. Kaneko, et al., *Phys.Rept.* **430**, 117 (2006), hep-ph/0308080.
- [78] M. A. Shifman, A. Vainshtein, M. Voloshin, and V. I. Zakharov, *Sov.J.Nucl.Phys.* **30**, 711 (1979).

- [79] M. Gavela, G. Girardi, C. Malleville, and P. Sorba, Nucl.Phys. **B193**, 257 (1981).
- [80] L. Bergstrom and G. Hulth, Nucl.Phys. **B259**, 137 (1985).
- [81] S. Chatrchyan et al. (CMS Collaboration), JHEP **1306**, 081 (2013), 1303.4571.
- [82] *ATLAS Collaboration*, <https://twiki.cern.ch/twiki/bin/view/AtlasPublic/SupersymmetryPublicResults>, CERN (2013) .
- [83] S. Chatrchyan et al. (CMS Collaboration), Eur.Phys.J. **C73**, 2677 (2013), 1308.1586.